Electromagnetic Turbulence Simulations of the Tokamak Scrape-Off Layer

F.D. Halpern, T.-M. Tran, F. Musil,
P. Ricci, F. Riva, C. Wersal

École Polytecnique Fédérale de Lausanne
Centre de Recherches en Physique des Plasmas
CH-1015 Lausanne, Suisse

June 3rd, 2015

A peek at the very edge of a tokamak plasma...

Visible light fluctuations at 400'000fps [S.Zweben (Princeton), J.Terry (MIT)]

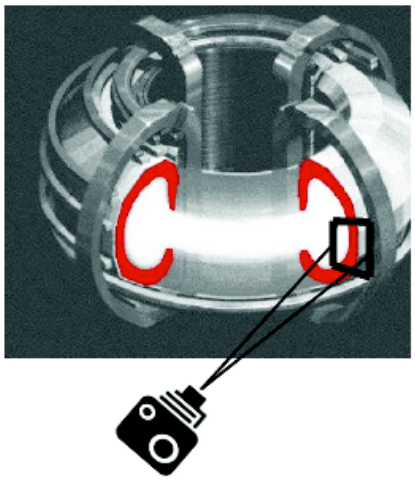

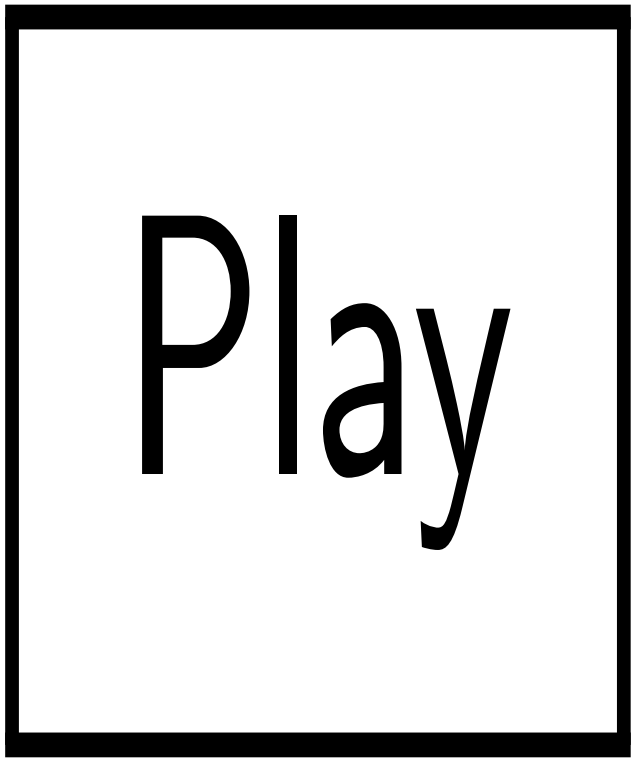

- Low temperature ($\sim$ 10eV) magnetized plasma
- Open B field lines $\rightarrow$ plasma not confined
- Low frequency modes $\omega \ll \omega_{ci}$
- $L_{fluc} \sim L_{eq}$
- $n_{fluc} \sim n_{eq}$

How do we develop an understanding of SOL dynamics?

Heat load to PFCs, rotation, impurities, L-H transition...

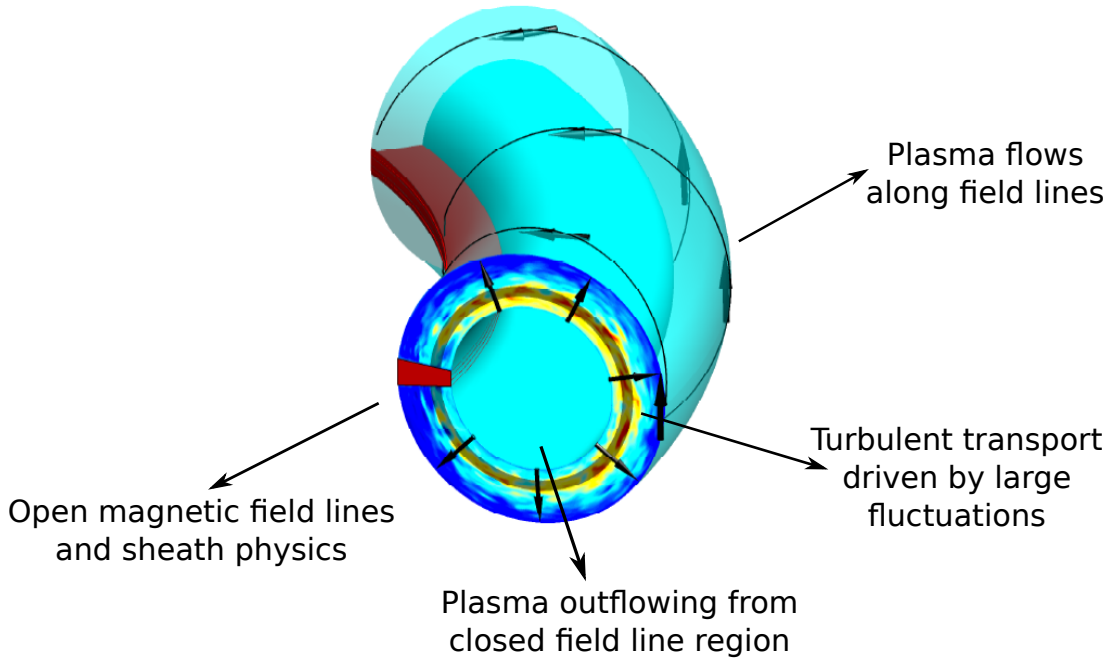

- GBS code: drift-reduced Braginskii eqns., flux-driven
- Full power balance $\rightarrow$ profile formation, $\lambda_q \rightarrow$ heat-flux length
- Good scaling up to medium size tokamak [Halpern, NF/PPCF (2013-14)]

Towards the next generation SOL turbulence code...

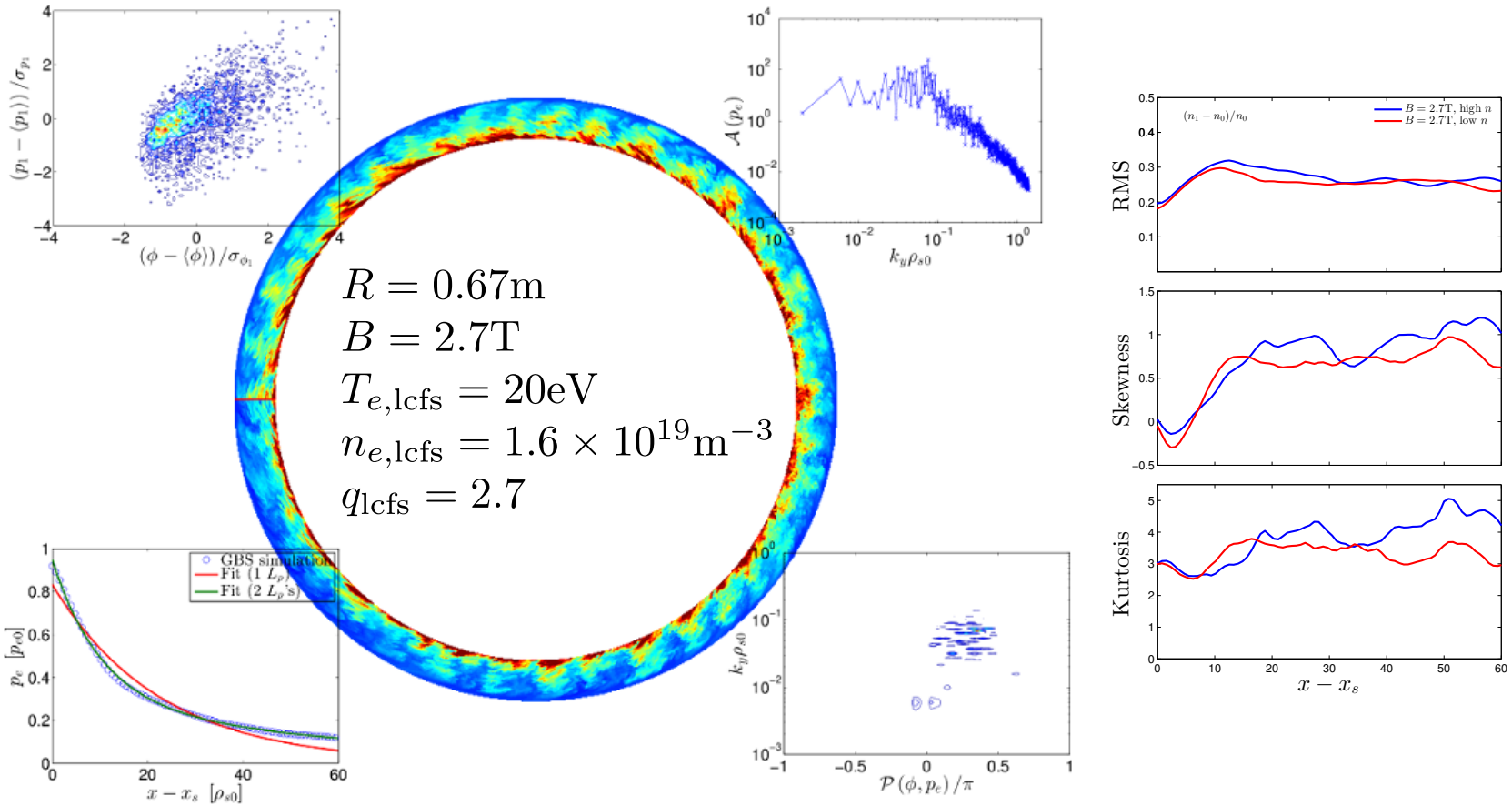

- Larger simulations required for experimental comparison
- Main roadblock to larger plasma sizes is Poisson solver

Drift-reduced Braginskii equations to describe the SOL

$$\frac{\partial n}{\partial t} = -\frac{\rho_\star^{-1}}{B}[\phi, n] + \frac{2}{B}\left[nC(T_e) + T_e C(n) - nC(\phi)\right] - n\nabla_\parallel v_{\parallel e} - v_{\parallel e}\nabla_\parallel n$$

$$\frac{\partial \tilde{\omega}}{\partial t} = -\frac{\rho_\star^{-1}}{B}[\phi, \tilde{\omega}] - v_{\parallel i}\nabla_\parallel \tilde{\omega} + \frac{B^2}{n}\nabla_\parallel j_\parallel + \frac{2B}{n}C(p) + \frac{B}{3n}C(G_i), \quad \tilde{\omega} = \nabla_\perp^2(\phi + \tau T_i)$$

$$\frac{\partial}{\partial t}\left(v_{\parallel e} + \frac{m_i}{m_e}\frac{\beta_e}{2}\psi\right) = -\frac{\rho_\star^{-1}}{B}[\phi, v_{\parallel e}] - v_{\parallel e}\nabla_\parallel v_{\parallel e} + \frac{m_i}{m_e}\left[\nu j_\parallel / n + \nabla_\parallel \phi - \frac{\nabla_\parallel p_e}{n} - 0.71\nabla_\parallel T_e - \frac{2}{3n}\nabla_\parallel G_e\right]$$

$$\frac{\partial v_{\parallel i}}{\partial t} = -\frac{\rho_\star^{-1}}{B}[\phi, v_{\parallel i}] - v_{\parallel i}\nabla_\parallel v_{\parallel i} - \frac{2}{3}\nabla_\parallel G_i - \frac{1}{n}\nabla_\parallel p$$

$$\frac{\partial T_e}{\partial t} = -\frac{\rho_\star^{-1}}{B}[\phi, T_e] - v_{\parallel e}\nabla_\parallel T_e + \frac{4}{3}\frac{T_e}{B}\left[\frac{7}{2}C(T_e) + \frac{T_e}{n}C(n) - C(\phi)\right] + \\ + \frac{2}{3}\left\{T_e\left[0.71\nabla_\parallel v_{\parallel i} - 1.71\nabla_\parallel v_{\parallel e}\right] + 0.71\,T_e(v_{\parallel i} - v_{\parallel e})\frac{\nabla_\parallel n}{n}\right\} + \mathcal{D}^\parallel_{T_e}(T_e)$$

$$\frac{\partial T_i}{\partial t} = -\frac{\rho_\star^{-1}}{B}[\phi, T_i] - v_{\parallel i}\nabla_\parallel T_i + \frac{4}{3}\frac{T_i}{B}\left[C(T_e) + \frac{T_e}{n}C(n) - C(\phi)\right] + \\ + \frac{2}{3}T_i\left(v_{\parallel i} - v_{\parallel e}\right)\frac{\nabla_\parallel n}{n} - \frac{2}{3}T_i\nabla_\parallel v_{\parallel e} - \frac{10}{3}\frac{T_i}{B}C(T_i) + \mathcal{D}^\parallel_{T_i}(T_i)$$

+Sheath BCs consistent with PIC simulations [Loizu, PoP (2012)]

+Equations for neutral ion physics [Wersal, to be submitted]

Status of GBS circa 2014 [Ricci, PPCF (2012)]

- 2nd order FD spatial discretization, RK4 time advance
- Arakawa scheme for $\mathbf{E} \times \mathbf{B}$ n.l. advection terms
- Field-aligned parallel gradient operators
- MPI domain decomposition in (x, z) directions
- Sparse linear solver for elliptical operators $\sim \nabla_\perp^2 \phi$
- Reasonable scalability up to medium size tokamak
  - $(ny, nx, nz) = (1384, 128, 256)$, $\Delta t = 10^{-5} R/c_s \sim 1sec$

Summary of new features in GBS

	Circa 2014	New GBS
Language	Fortran90	F2003/8
Parallelization	2-D MPI DD (z, x)	3-D MPI DD (z, y, x)
Elliptical solver	Parallel sparse	Parallel multigrid
Scalability	$\sim$1024 cores	$\sim$8192 cores
ES potential	$\nabla\cdot(n\nabla_\perp\phi) \sim \nabla^2_\perp\phi/n$ (Boussinesq)	Retain full $\tilde{\phi} \leftrightarrows \tilde{n}$ coupling
EM effects	Small plasma size	Arbitrary size

- Also: Ongoing effort to port GBS to manycore/GPU architecture using OpenMP/OpenACC/MPI (2016)

Stencil based parallel multigrid implemented in GBS

- 2D Cartesian (x, y) grid topology mapped to a 2D domain decomposition

$$\mathbf{D}_i = \begin{pmatrix} \delta_{xy,(-1,1)} & \delta_{yy(0,1)} & \delta_{xy,(1,1)} \\ \delta_{xx,(-1,0)} & \delta_{xx(0,0)} + \delta_{yy(0,0)} & \delta_{xx,(1,0)} \\ \delta_{xy,(-1,-1)} & \delta_{yy(0,-1)} & \delta_{xy,(1,-1)} \end{pmatrix}$$

$$\mathbf{R}_i = \frac{1}{16}\begin{pmatrix} 1 & 2 & 1 \\ 2 & 4 & 2 \\ 1 & 2 & 1 \end{pmatrix}, \qquad \mathbf{I}_{i,x} = \frac{1}{2}\begin{pmatrix} 1 & 1 \end{pmatrix}, \qquad \mathbf{I}_{i,y} = \frac{1}{2}\begin{pmatrix} 1 \\ 1 \end{pmatrix}$$

- Use $\delta_{\alpha\beta}$ to describe diagonally dominant 2-D elliptic operators
  - Including plasma shaping, generalized Poisson operators,...
- Damped Jacobi/RB Gauss-Seidel/SOR relaxation
- In GBS, we converge the residue to $\varepsilon \sim 10^{-10}$ within 3-4 V(3,3)-cycles

Turbulent steady state successfully verified

- Compare steady state profiles, fluctuation moments...

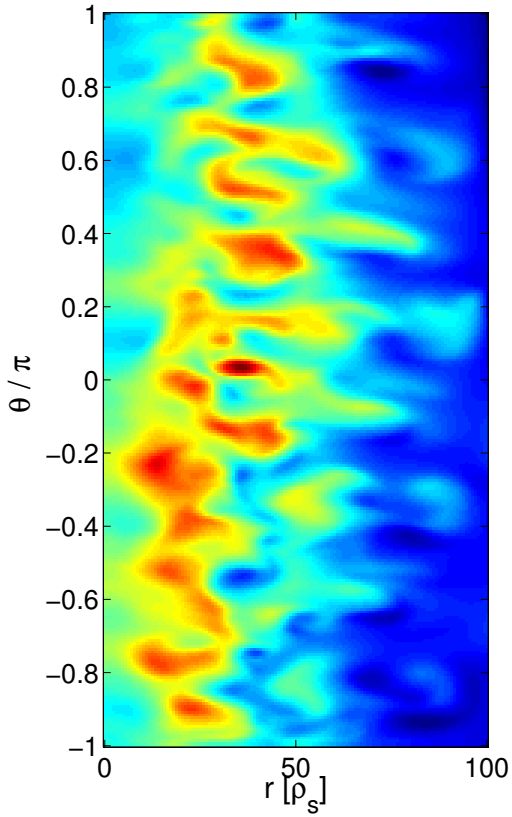

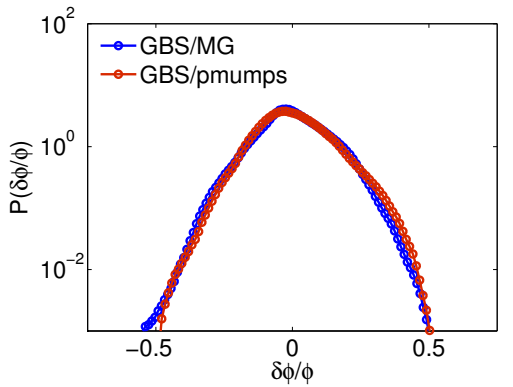

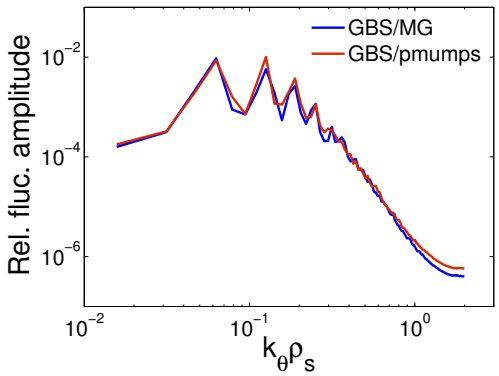

Parallel benchmarks show improved performance/scalability

- Compare GBS strong/weak scalings in PizDaint:
  parallel multigrid vs pmumps backsolve

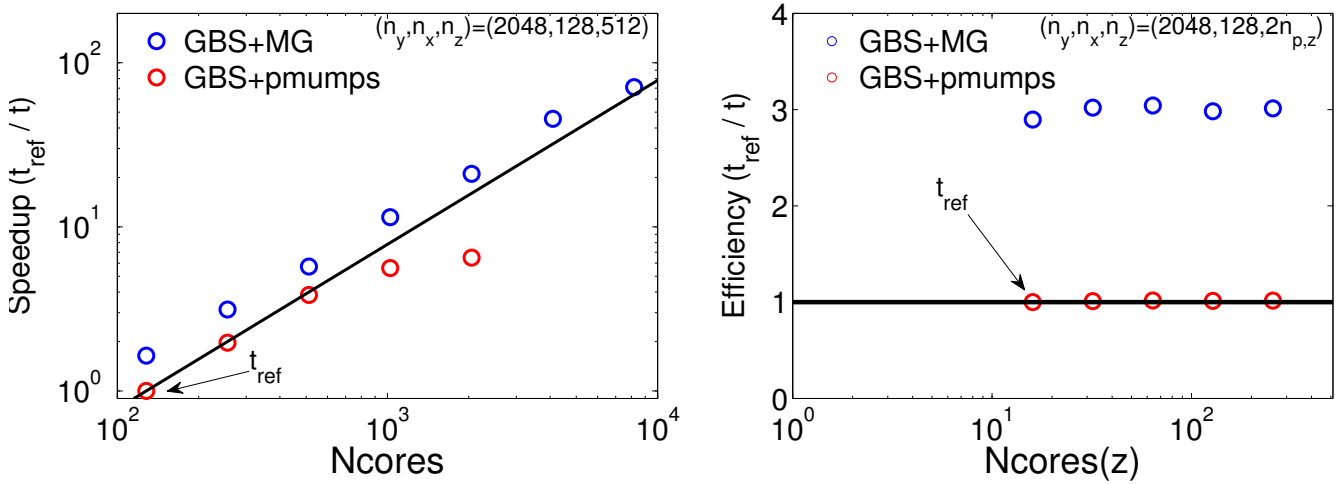

- New GBS scales up to ∼8192 cores for large plasmas
  - Parallel multigrid solver yields better performance at any size

Electromagnetic effects now possible at large size

New multigrid solver allows efficient inversion of time dependent operators:

- Ampère's equation from Ohm's law including electron inertia

$$\frac{\partial}{\partial t}\left(v_{\parallel e}+\frac{\beta_e}{2}\frac{m_i}{m_e}\psi\right)=\ldots$$

$$\Rightarrow\left[\nabla_\perp^2-\frac{\beta_e}{2}\frac{m_i}{m_e}n(y,x,z,t)\right]v_{\parallel e}=S_{v_{\parallel e}}$$

- Severe disadvantages of direct inversion removed in new GBS
  - No need to LU decompose regularly (computational cost)
  - Memory limits plasma size because of matrix size

Extended weak scaling including EM effects

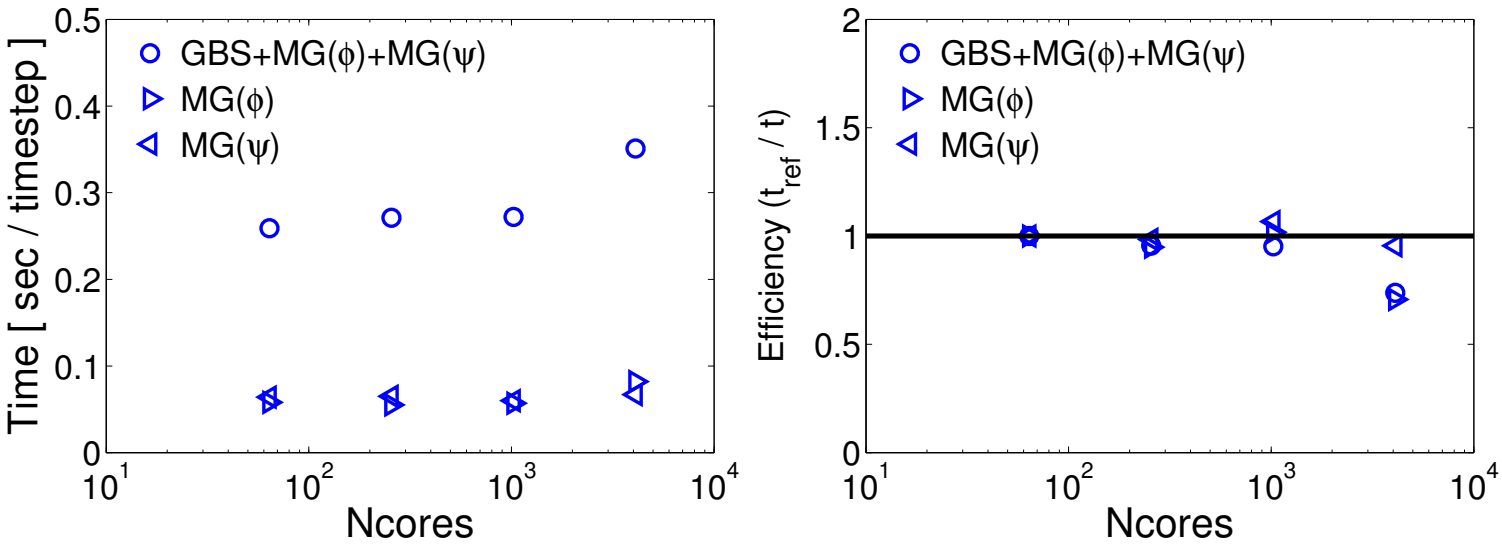

- Here, the plasma volume was increased by a factor of 64
- Multigrid solution time does not degrade with core number
- Modest cost increase respect to ES simulations

Boussinesq approximation removed from GBS

- The Boussinesq approximation

$$[\nabla \cdot (n(y,x,z,t)\nabla_\perp)]\,\phi \sim \nabla_\perp^2 \phi / n(y,x,z,t)$$

  is not really justifiable in the tokamak SOL $\rightarrow \delta n/n \sim \mathcal{O}(1)$

- We have reformulated drift-reduced Braginskii eqns to obtain new vorticity equation retaining full (n, ϕ) coupling

$$\begin{aligned} \frac{d\tilde{\omega}}{dt} &= \nabla \cdot (j_\star + j_\parallel)\,/n & \Rightarrow \frac{d\Omega}{dt} &= \nabla \cdot (j_\star + j_\parallel) \\ \tilde{\omega} &= \nabla \cdot (\nabla_\perp \phi + \tau \nabla_\perp T_i) & \Rightarrow\ \Omega &= \nabla \cdot (n\nabla_\perp \phi + \tau \nabla_\perp p_i) \end{aligned}$$

- Implemented in GBS using finite volume stencil for ϕ

$$\int \Omega dV = \int \nabla \cdot (n\nabla_\perp \phi)\, dV \rightarrow \int n\,(\nabla_\perp \phi \cdot \hat{n})\, dl$$

First Non-Boussinesq simulations now complete

We already start to see some differences in the plasma dynamics...

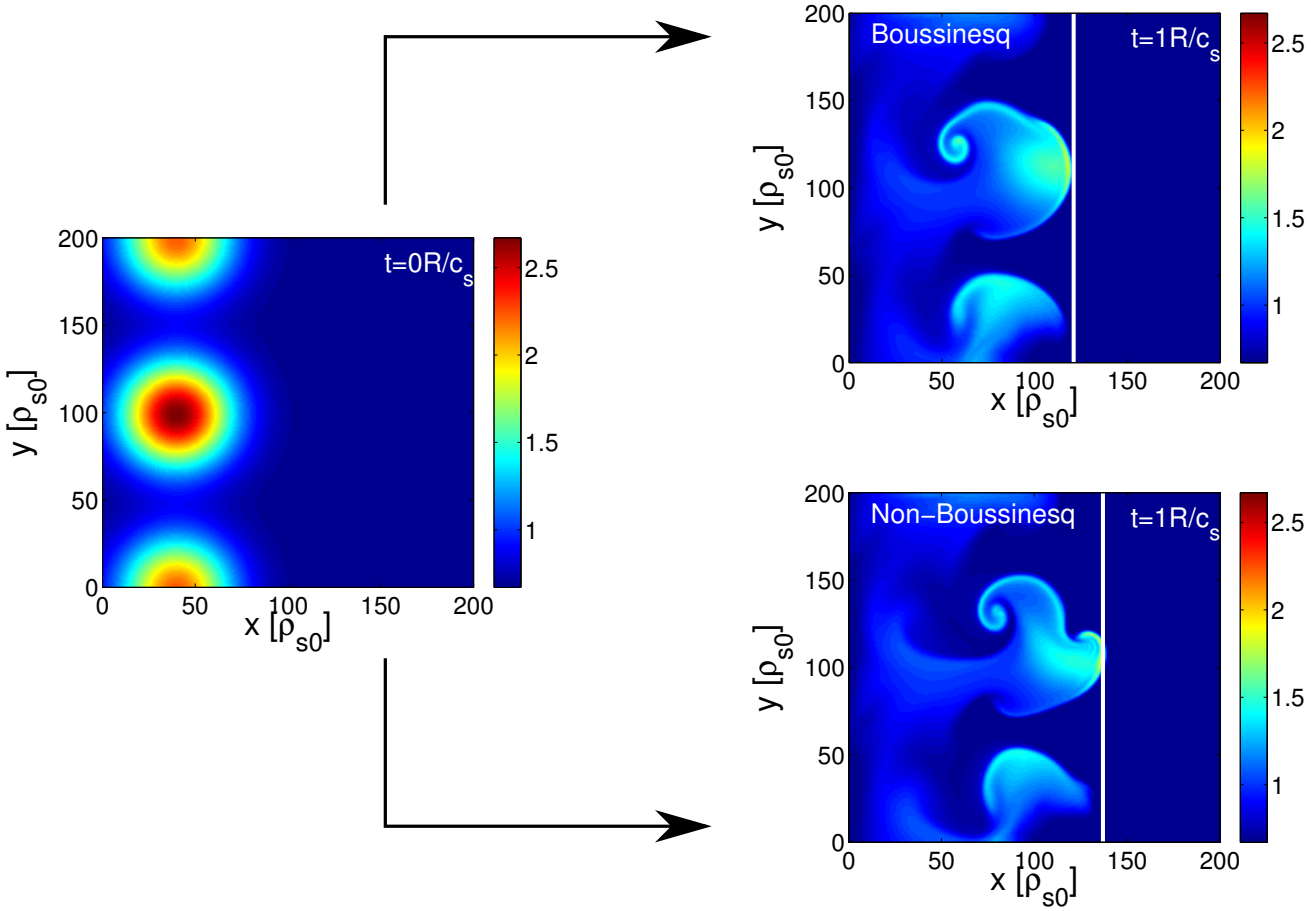

CRPP

Summary and conclusions

- First production runs with new GBS version now ongoing
- Code updated to F2003/8, pure MPI parallelism upgraded
- Poisson solver rewritten using multigrid techniques
- Main accomplishements:
  - EM runs at large size $\rightarrow$ size scaling of magnetic flutter effects
  - Non-Boussinesq equations $\rightarrow$ study flow/turbulence interaction
  - Typical simulation cost cut by half, walltime cut by factor of 4

Outlook and future work

- Benchmarking of stencil operators for MG carried out using OpenMP/OpenACC/MPI
- Begin porting Poisson solver to MPI/OpenMP hybrid

Extra slides

The Stencil Kernel

- Experiment with kernel computation (9-point stencil)
- OpenMP and OpenACC parallelization (single node)

```
1  !$omp parallel do private(ix,iy)
2  !$acc parallel loop present(mat,x,y) private(ix,iy)
3      DO iy=0,ny
4          DO ix=0,nx
5              y(ix,iy) =  mat(ix,iy,1)*x(ix-1,iy-1) &
6                   &    + mat(ix,iy,2)*x(ix,  iy-1) &
7                   &    + mat(ix,iy,3)*x(ix+1,iy-1) &
8                   &    + mat(ix,iy,4)*x(ix-1,iy  ) &
9                   &    + mat(ix,iy,0)*x(ix  ,iy  ) &
10                  &    + mat(ix,iy,5)*x(ix+1,iy  ) &
11                  &    + mat(ix,iy,6)*x(ix-1,iy+1) &
12                  &    + mat(ix,iy,7)*x(ix  ,iy+1) &
13                  &    + mat(ix,iy,8)*x(ix+1,iy+1)
14          END DO
15      END DO
16 !$acc end parallel loop
17 !$omp end parallel do
```

Performance on Piz Daint (Cray XC30)

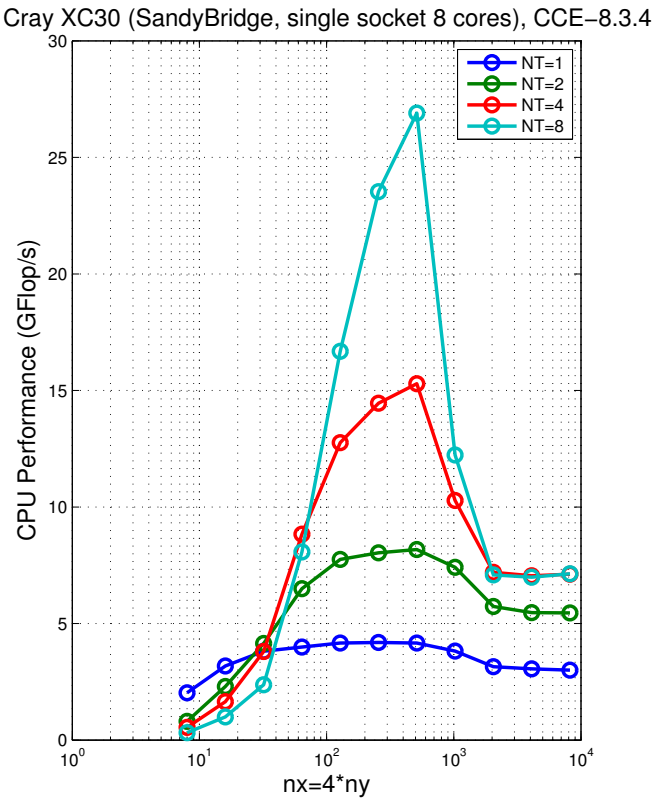

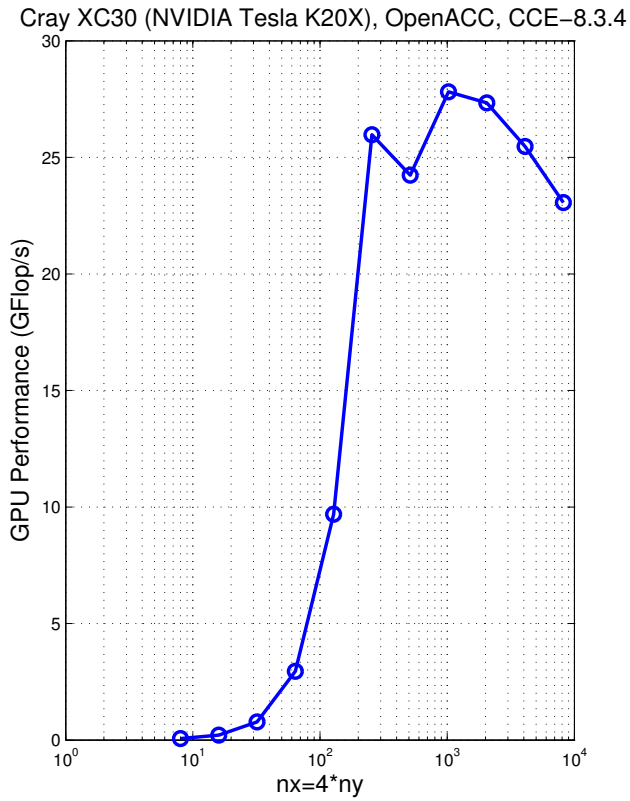

- NVIDIA GPU 3× faster than 8 CPU cores for $(nx, ny) > 1024 \times 256$
- Small flop intensity per thread in smaller grids.

Performance on Helios

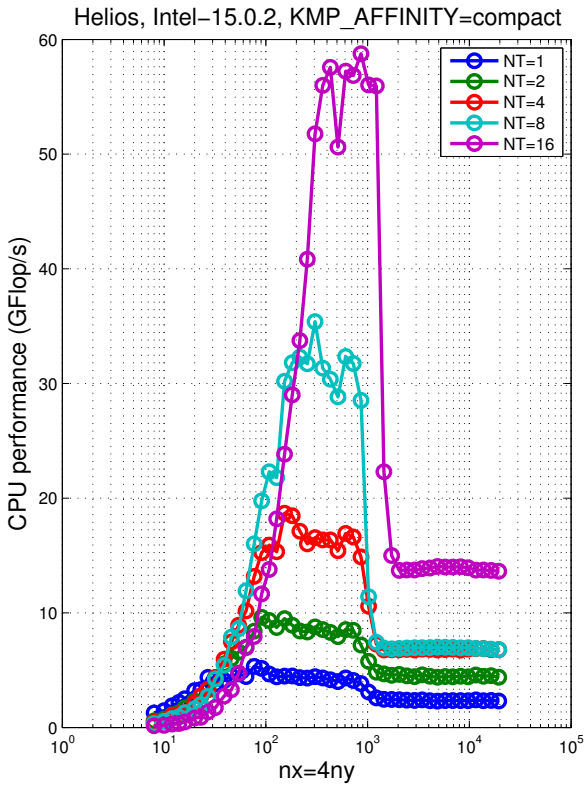

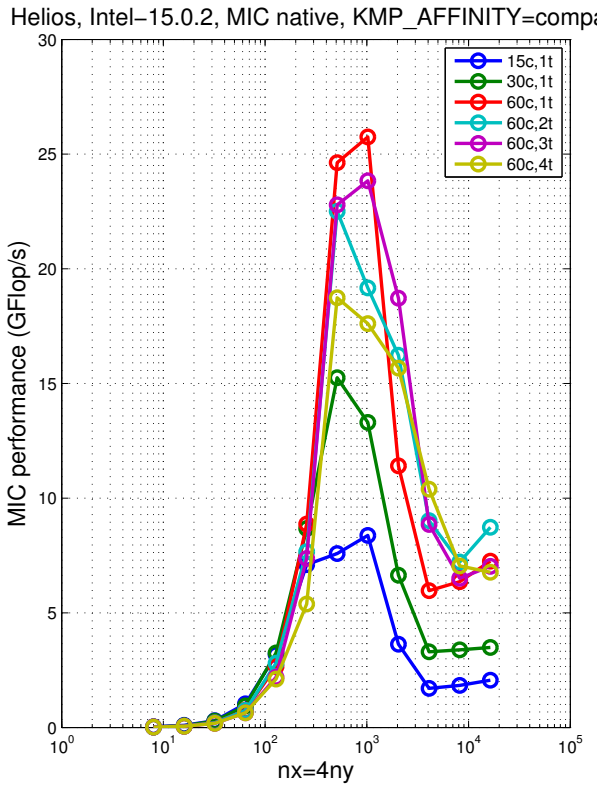

- Good parallel speedup on host CPU
- MIC scales only up to 60 cores with 1 thread/core
- MIC performance not better than 8 CPU cores

Performance on Helios (cont.)

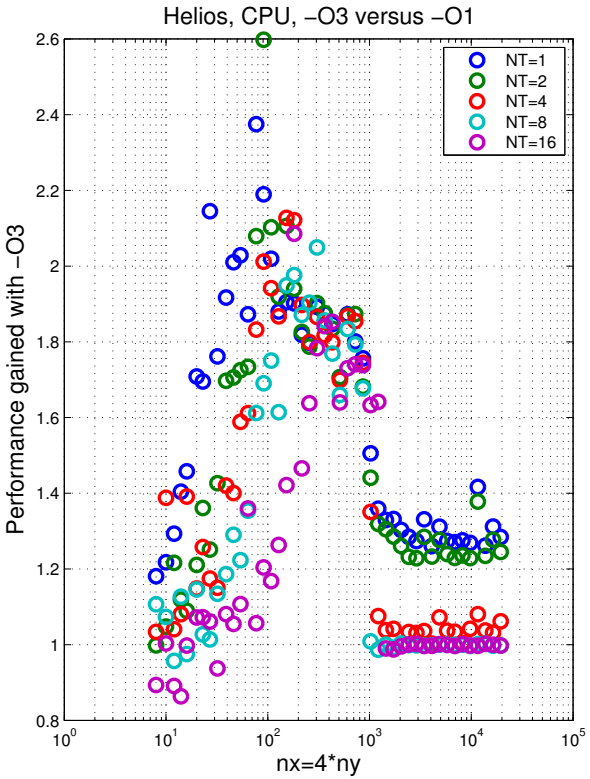

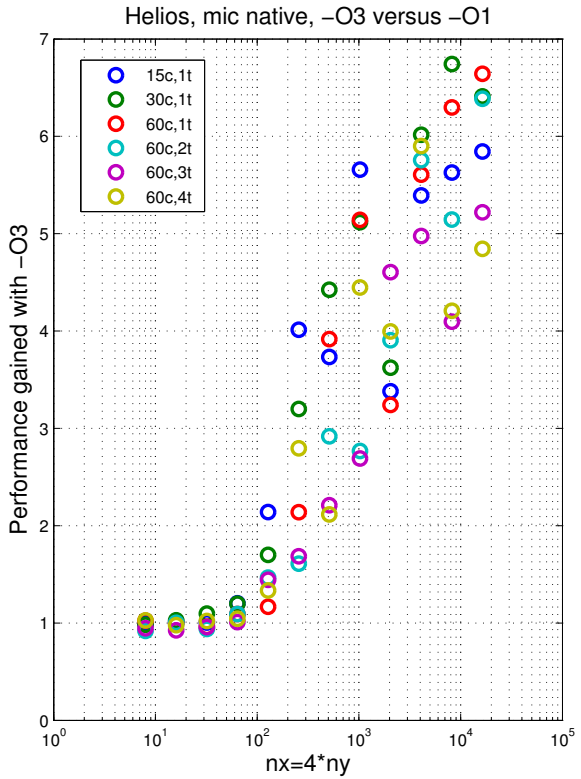

- Good vector speedup on both CPU and MIC
- Poor parallel performance on MIC: overhead of creation of large number of threads?

Sheath boundary conditions from kinetic approach

- COLLISIONAL PRESHEATH (**CP**)
  - Quasi-neutral, IDA holds
  - Potential drop $\sim 0.5 T_e$ over $\sim$ L
  - Ions accelerated to $v_s = c_s \sin\alpha$
- MAGNETIC PRESHEATH (**MP**)
  - Quasi-neutral, IDA breaks
  - Potential drop $\sim 0.5 T_e$ over $\sim \rho$
  - Ions accelerated to $v_s = c_s$
- DEBYE SHEATH (**DS**)
  - Non-neutral, IDA breaks
  - Potential drop $\sim 3 T_e$ over ~ 10
  - Ions accelerated to $v_s > c_s$

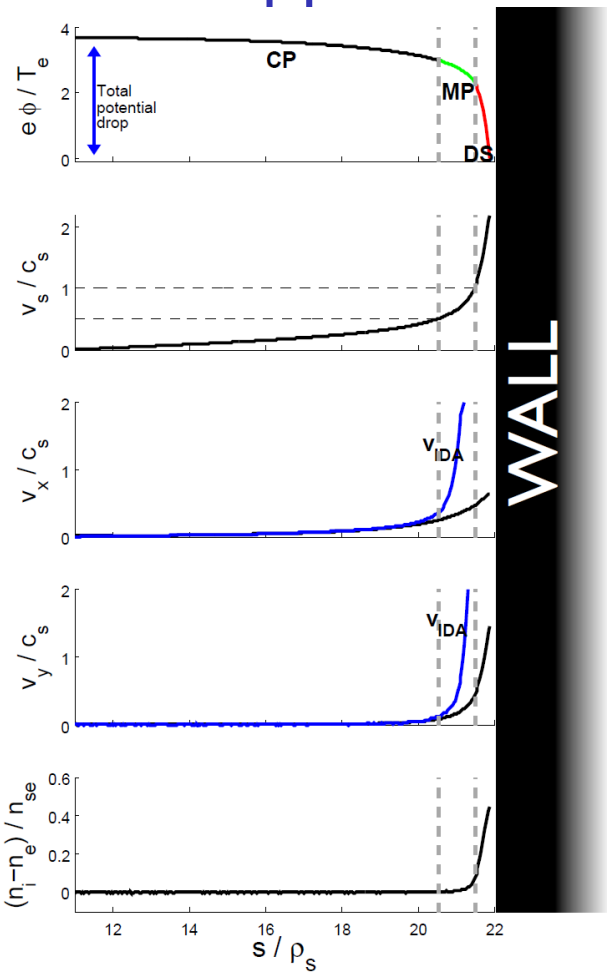

Fluid BCs at the Magnetic Pre-Sheath Entrance:

$$v_{||i} = \pm c_s \left(1 + \theta_n - \frac{1}{2}\theta_{T_e} - \frac{2\phi}{T_e}\theta_\phi\right)$$

$$v_{||e} = \pm \sqrt{T_e}\left(\exp\left(\Lambda - \eta_m\right) - \frac{2\phi}{T_e}\theta_\phi + 2(\theta_n + \theta_{T_e})\right)$$

$$\frac{\partial \phi}{\partial y} = \mp c_s \left(1 + \theta_n + \frac{1}{2}\theta_{T_e}\right)\frac{\partial v_{||i}}{\partial y}$$

$$\frac{\partial n}{\partial y} = \mp \frac{n}{c_s}\left(1 + \theta_n + \frac{1}{2}\theta_{T_e}\right)\frac{\partial v_{||i}}{\partial y}$$

$$\frac{\partial T_e}{\partial y} = \frac{\partial T_i}{\partial y} \simeq 0$$

$$\tilde{\omega} = -\cos^2\alpha\left[\left(1 + \theta_{T_e}\right)\left(\frac{\partial v_{||i}}{\partial y}\right)^2 + c_s\left(1 + \theta_n + \theta_{T_e}/2\right)\frac{\partial^2 v_{||i}}{\partial y^2}\right]$$

where $\theta_A = \frac{\rho_s}{2\tan\alpha}\frac{\partial_x A}{A}$, and $\eta_m = e(\phi_{mpe} - \phi_{wall})/T_e$. [Loizu et al PoP 2012]